TELECOM
ParisTech

Comparative study of reuse patterns for WiMAX cellular networks

Comparaison de différents schémas de réutilisation fréquentielle pour les réseaux cellulaires WiMAX

Masood Maqbool
Marceau Coupechoux
Philippe Godlewski

2008D005

Avril 2008

Département Informatique et Réseaux
Groupe RMS : Réseaux, Mobilité et Sécurité

Comparative Study of Reuse Patterns for WiMAX Cellular Networks

Comparaison de différents schémas de réutilisation fréquentielle pour les réseaux cellulaires WiMAX

Masood Maqbool, Marceau Coupechoux, Philippe Godlewski

Département Informatique et Réseaux

TELECOM ParisTech

Contents

List of Figures

List of Tables

List of Acronyms

AMC	Adaptive Modulation and Coding
AWGN	Additive White Gaussian Noise
BER	Bit Error Rate
BS	Base Station
BW	Bandwidth
BWA	Broadband Wireless Access
DL	Downlink
EESM	Exponential Effective SINR Mapping
FEC	Forward Error Correction
FFT	Fast Fourier Transform
FUSC	Full Usage of Subchannels
GEV	Generalized Extreme Value
LLS	Link Level Simulation
MCS	Modulation and Coding Scheme
MIC	Mean Instantaneous Capacity
OFDM	Orthogonal Frequency Division Multiplex
OFDMA	Orthogonal Frequency Division Multiple Access
PER	Packet Error Rate
PDF	Probability Density Function
PHY	Physical
PUSC	Partial Usage of Subchannels
SINR	Signal to Noise and Interference Ratio

$SINR_{eff}$	Effective Signal to Noise and Interference Ratio
SLS	System Level Simulation
SS	Subscriber Station
UL	Uplink
WiMAX	Worldwide Interoperability for Microwave Access

1 Introduction

IEEE 802.16 standard is intended to pave a way towards rapid worldwide deployment of cost-effective and interoperable Broadband Wireless Access (BWA) products. Worldwide Interoperability for Microwave Access (WiMAX) proposed by WiMAX Forum is based on IEEE 802.16 standard. WiMAX has two types: fixed and mobile. The purpose of this article is to study the effect of six different reuse factors on radio quality and capacity in a mobile WiMAX network. Radio quality is analyzed in terms of Effective Signal to Noise and Interference Ratio ($SINR_{eff}$) vesus distance and $SINR_{eff}$/MCS distributions. The rest of the sections are introduced hereafter.

In section-2 details are given about the radio quality parameters and capacity of a WiMAX network. Per subcarrier SINR formula is described. The purpose to calculate $SINR_{eff}$ is explained. Physical abstraction models Mean Instantaneous Capacity (MIC) and Exponential Effective SINR Mapping (EESM) are described. Process to calculate capacity, $SINR_{eff}$ and MCS distributions are also illustrated.

Details about network simulator are given in section-3. Wraparound method used in the simulations has been explained. This section also includes parameter values (as given in [3]) used in simulations. Introduction to six different reuse patterns is also covered in this section.

Section-4 spans the results obtained in simulations followed by conclusion. Conclusion is based on the comparison between results obtained from six different reuse patterns.

Effect of variable cell range and subcarrier is analyzed in section-5 which is followed by section-6 concluding this report.

2 Radio Quality Parameters and Capacity

2.1 Introduction

In this section details about radio quality parameters and capacity in a WiMAX cellular network are given. As already narrated in section-1, we

shall consider two radio quality parameters namely: $SINR_{eff}$ and MCS distribution. $SINR_{eff}$ can be determined using various PHY abstraction models. The need of these PHY abstraction models is also explained in this section. Details about two PHY abstraction models (MIC and EESM) are also given. Relationship between SLS and LLS has also been detailed. We shall start with the description of SINR computation.

2.2 Signal to Noise and Interference Ratio (SINR)

In order to calculate subcarrier SINR for a Subscriber Station (SS) at a distance d from the BS, following formula is used:

$$SINR_n = \frac{P_{n,Tx} a_{n,SH}^{(0)} a_{n,FF}^{(0)} \frac{K}{d^{(0)\alpha}}}{N_0 W_{SC} + \sum_{j=1}^{B} P_{n,TX} a_{n,SH}^{(j)} a_{n,FF}^{(j)} \frac{K}{d^{(j)\alpha}} \delta_n^{(j)}}$$

(1)

Where

n is the subcarrier index.

W_{SC} is the subcarrier spacing.

N_0 is the thermal noise density.

$P_{n,Tx}$ is the per subcarrier power in DL (cf. subsection-3.7).

$a_{n,SH}^{(0)}$ is the shadowing factor for subcarrier n.

$a_{n,FF}^{(0)}$ is the fast fading factor for subcarrier n.

B is the number of interfering BS.

K is the pathloss constant.

α is the pathloss exponent.

$d^{(0)}$ is the distance of SS (subscriber station) from serving BS.

$a_{n,SH}^{(j)}$ is the shadowing factor for subcarrier n w.r.t interfering BS j.

$a_{n,FF}^{(j)}$ is the fast fading factor for subcarrier n w.r.t interfering BS j.

$d^{(j)}$ is the distance of SS from interfering BS j.

$\delta_n^{(j)}$ is equal to 1 if interfering BS transmits on n^{th} subcarrier and 0 otherwise.

2.2.1   Effective SINR

Using LLS, average SINR vs BER/PER curves can be obtained. There are three inputs to LLS module: average SINR, MCS and channel model. Output of this module is BER/PER (Fig.1). Simulations are carried out using different values of average SINR as inputs. The corresponding output BER/PER values are plotted against those input values. For different MCS types/channel models, a number of average SINR vs BER/PER curves are obtained.

On the other hand, SLS takes propagation model, cell configuration and network layout as inputs and outputs average SINR (Fig.1). This value of average SINR is mapped to the curves of LLS to find BER/PER. Following text gives two approaches to reach this result.

One possibility is to find SINR values of all the radio links (for all subcarriers) that are present between all the SS and all the BS (for different MCS types/channel models) through SLS. Then by running the LLS, SINR vs BER/PER curves are obtained for all above radio links. Finally SINR values obtained through SLS are mapped to the curves obtained from LLS to find BER/PER [4]. The computational load involved in this process is apparent. We shall refer this possibility as high computational method in the following text.

The second approach is to use a PHY abstraction model to calculate an
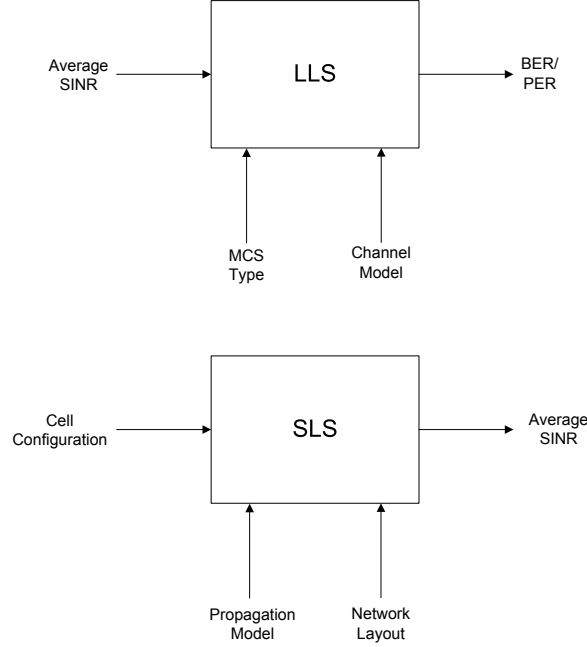
Figure 1: Link level and system level simulations' modules

average SINR value over a number of subcarriers through SLS. The PHY abstraction model is expected to find such an average value of SINR that can be mapped (to LLS curves) through a performance metric which is not link dependent. This link independent performance metric is typically SINR in AWGN conditions. The SINR vs BER/PER curves in AWGN conditions can be easily generated using simple simulations and analytical formulas. Therefore the function of PHY abstraction model is to find that value of SINR (called $SINR_{eff}$), which if mapped to these AWGN curves, gives the same result as if it was obtained using high computational method. One additional benefit of this technique is that AWGN curves are available offline.

PHY Abstraction models average the SINR of a number of subcarriers (the choice of this number is with the user). However, this is not a arithmetic averaging and reasons for this as given in [3] are:

1. The bits of FEC (forward error correction) block are spread over different subcarriers

4

2. At the receiver end, aside from average SINR, decoder behavior also depends on the SINR fluctuations between subcarriers (carrying FEC block bits). Even the bursts (observing different channel and interference characteristics) with same average SINR values will show different BER/PER results.

Few PHY abstraction models presented in [3] are named as follows:

- Average SNR

- Mean instantaneous capacity (MIC)

- Effective SINR

- Exponential effective SINR mapping (EESM) etc.

Because of simplicity, we have chosen MIC as a PHY abstraction model for our SLS of a WiMAX network. In this report, EESM and MIC models are illustrated. Out of BER/PER, PER has been chosen as the required output. All the steps involved in two models are listed. However, in network simulations only $SINR_{eff}$ (using MIC) has been calculated. Details about the comparison of these two abstraction models can be found in [7].

Exponential Effective SINR Mapping (EESM)

The first step is to calculate SINR of nth subcarrier for a given user at a given position using Eq.1.

Next, $SINR_{eff}$ is computed by Eq.2 [3] using the instantaneous values of SINR of first step.

$$SINR_{eff} = -\beta \cdot \ln \left(\frac{1}{N'} \sum_{n=1}^{N'} e^{-\frac{SINR_n}{\beta}} \right) \tag{2}$$

Where

$SINR_n$ is the SINR value of the nth subcarrier.

β is an adjustment factor that depends on the FEC type, MCS and receiver implementation. It is obtained through LLS.

N' is the number of subcarriers over which $SINR_{eff}$ is computed.

Finally PER is computed from a table or a curve function determined in advance (from LLS) for basic AWGN channel associated with given $SINR_{eff}$ from step two and the current used MCS [3]:

$$PER = F_{AWGN}(SINR_{eff}, MCS)$$

Mean Instantaneous Capacity (MIC)

The first step is the same as that for EESM, i.e., to calculate SINR of nth subcarrier for a given user at a given position.

Next step is to compute capacity for n^{th} subcarrier using Shannon's formula:

$$C_n = \log_2\left(1 + SINR_n\right) \quad [bps/Hz]$$

Now using the values of capacity, MIC is computed by averaging capacities of N' subcarriers:

$$MIC = \frac{1}{N'} \sum_{n=1}^{N'} C_n \quad [bps/Hz]$$

PER is computed from a table or a curve function determined in advance (from LLS) for basic AWGN channel associated with given MIC (from step two) and the current used MCS [3]:

$$PER = F_{AWGN}(SINR_{eff}, MCS)$$

At the end $SINR_{eff}$ is obtained from MIC value using following equation:

$$SINR_{eff} = 2^{MIC} - 1 \qquad (3)$$

2.3   WiMAX Capacity

Since we shall carry out system simulations in DL only, the analytical calculation of DL capacity of a WiMAX network are presented here. MIC value is calculated per Hz. In order to obtain the equivalent capacity of a subcarrier, we have to multiply this MIC value with subcarrier frequency spacing.

$$Subcarrier\ capacity \quad = \quad Subcarrier\ spacing \times MIC \quad [bps]$$

Basic data unit of a WiMAX system is a slot. The number of bits in one slot is computed as:

$$Slot\ Capacity \quad = \quad Slot\ duration \times No\ of\ subcarrier\ per\ slot$$
$$\times Subcarrier\ capacity \qquad [bits/slot]$$

There are multiple number of slots in a DL subframe. Also there are total 200 DL subframes (1/Frame duration) in one second. DL capacity is given as:

$$Capacity\ of\ DL\ subframe \quad = \quad Slot\ Capacity$$
$$\times No.\ of\ slots\ in\ DL\ subframe$$
$$\times \frac{1}{Frame\ Duration} \times Load\ Factor\ [bps]$$

Where

$$Load\ Factor = \frac{No.\ of\ used\ Subchannels}{Max.\ no.\ of\ Subchannels(DL)} \qquad (4)$$

7

The term *Load Factor* is used because of the fact that operator of a WiMAX can be given discretion to use only a part of total subchannels (for a given FFT size) in a given cell/sector. The rest of the subchannels are assigned to other cells/sectors. It will give an advantage of higher reuse factor and will result in better SINR values for users. But at the same time, capacity is decreased because of less number of subchannels.

3 Network Simulations

3.1 Introduction

In this section details about simulation of WiMAX network are given. Network layout (with different reuse factors), wraparound technique, spatial distribution of SS, sectorization, antenna diagram, etc, have been described. The parameter values used in simulations are also given. Monte Carlo simulations are carried (for subcarrier distributions PUSC) and simulation results are compared for different types of reuse patterns. It is to be noted that simulations are carried out in DL direction only and hence all the information in this section is customized accordingly.

3.2 Network Layout

A hexagonal cellular network is considered with length of one side of the hexagon equal to R. The simulations have been carried out using wraparound technique. As given in [3], network is divided into clusters. Each cluster consists of N_c number cells. There are N_s sectors and N_f different frequencies per cell. The reuse factor can therefore be depicted as N_c x N_s x N_f. The number of interfering BS for each reuse pattern is same. Six different reuse patterns (given in [3]) are presented in Fig.2 (copied from [3]).

3.3 Wraparound Technique

This text on wraparound method is based on [5] and [6]. We start with introduction of few terms. The symmetry in a hexagonal network means that one would not notice the difference when standing in the middle of the hexagon,
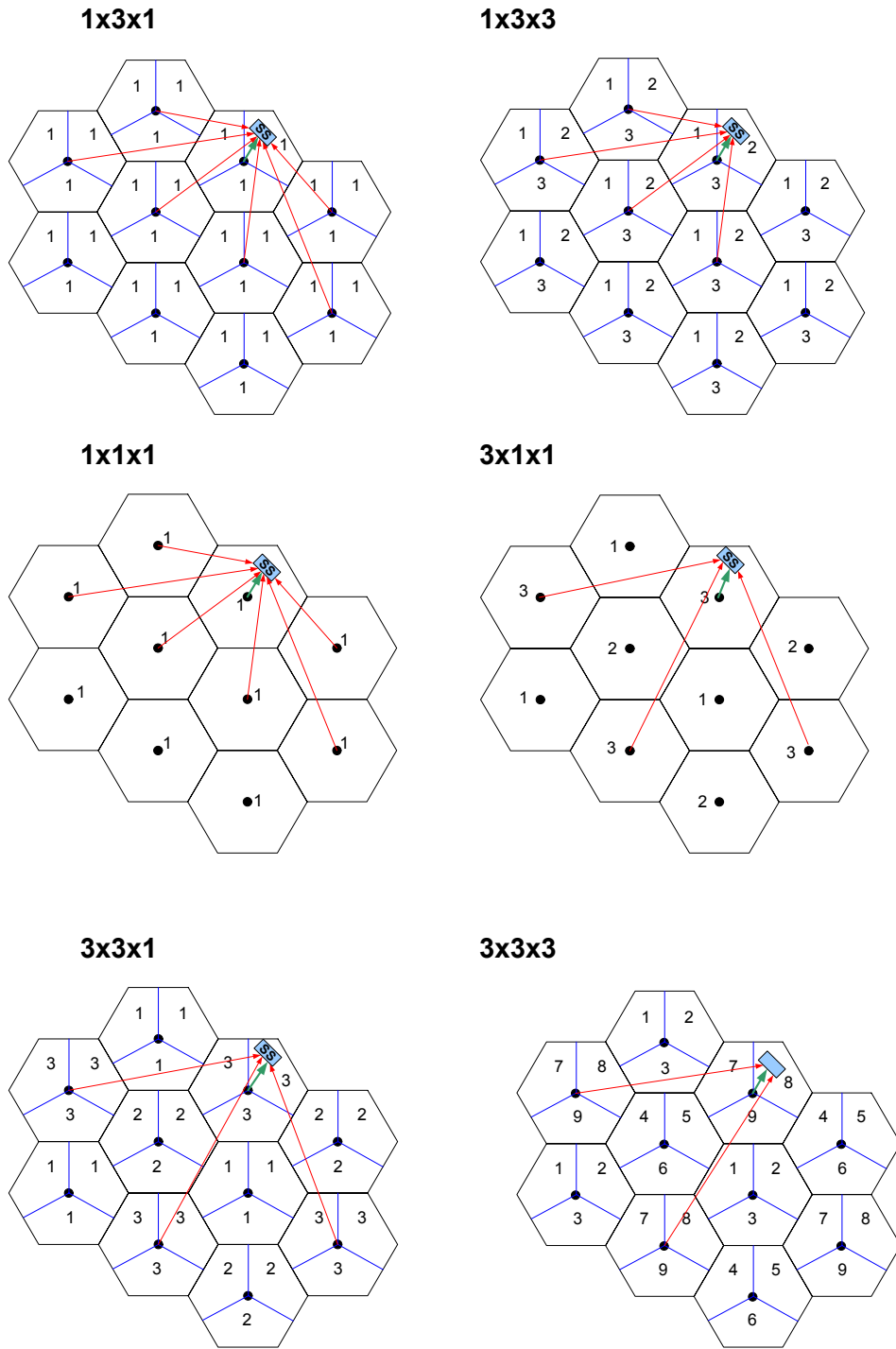
1x3x1

1x3x3

1x1x1

3x1x1

3x3x1

3x3x3

Figure 2: Six different reuse patterns for WiMAX Networks [3].

9

while the hexagon is rotated or reflected accordingly. In a two tier network with finite number of nodes, only the central cell enjoys such symmetry. In such a network only the data collected in the central cell will have statistical characteristics equivalent to a network consisting of infinite cells. Also to collect a large amount of data, it is desired to drop the SS in the cells other than the central one. To address this issue, idea of wraparound is introduced.

Using wraparound method, the network is extended to a cluster of network consisting of eight copies of the original hexagonal network. With the original hexagonal network in the middle, eight copies are attached to it symmetrically as shown in the Fig.3. This cell layout is wraparound to form a toroidal surface. In order to be able to perform this mapping, the number of cells in a cluster has to be a rhombic number. There is a one-to-one mapping between cells/sectors of the center hexagon and cells/sectors of each copy. In this way every cell in the extended network is identified with one of the cells in the central original network. Those corresponding cells have thus the same antenna configuration, traffic, fading, etc, except the location. This correspondence is shown in Fig.3 through shaded sectors of the same cell in all the networks.

Let us consider a two tier wraparound model. The signal or interference from any SS to a given cell is treated as if that SS is in the first 2 rings of neighboring cells. The distance from any SS to any BS is obtained as follows. A coordinate system is defined with center cell of original network at $(0,0)$. The path distance and angle used to compute the path loss and antenna gain of a SS at (x,y) to a BS at (a,b) is the minimum of the following:

Distance1 = Distance between (x,y) and (a,b)

Distance2 = Distance between (x,y) and $(a + 2.5\sqrt{3}D, b + D/2)$

Distance3 = Distance between (x,y) and $(a + \sqrt{3}D, b + 4D)$

Distance4 = Distance between (x,y) and $(a - \sqrt{3}D/2, b + 7.5D)$

Distance5 = Distance between (x,y) and $(a - 1.5\sqrt{3}D, b + 3.5D)$

Distance6 = Distance between (x,y) and $(a - 2.5\sqrt{3}D, b - D/2)$

10

Distance7 = Distance between (x, y) and $(a - \sqrt{3}D, b - 4D)$

Distance8 = Distance between (x, y) and $(a + \sqrt{3}D/2, b - 7.5D)$

Distance9 = Distance between (x, y) and $(a + 1.5\sqrt{3}D, b - 3.5D)$

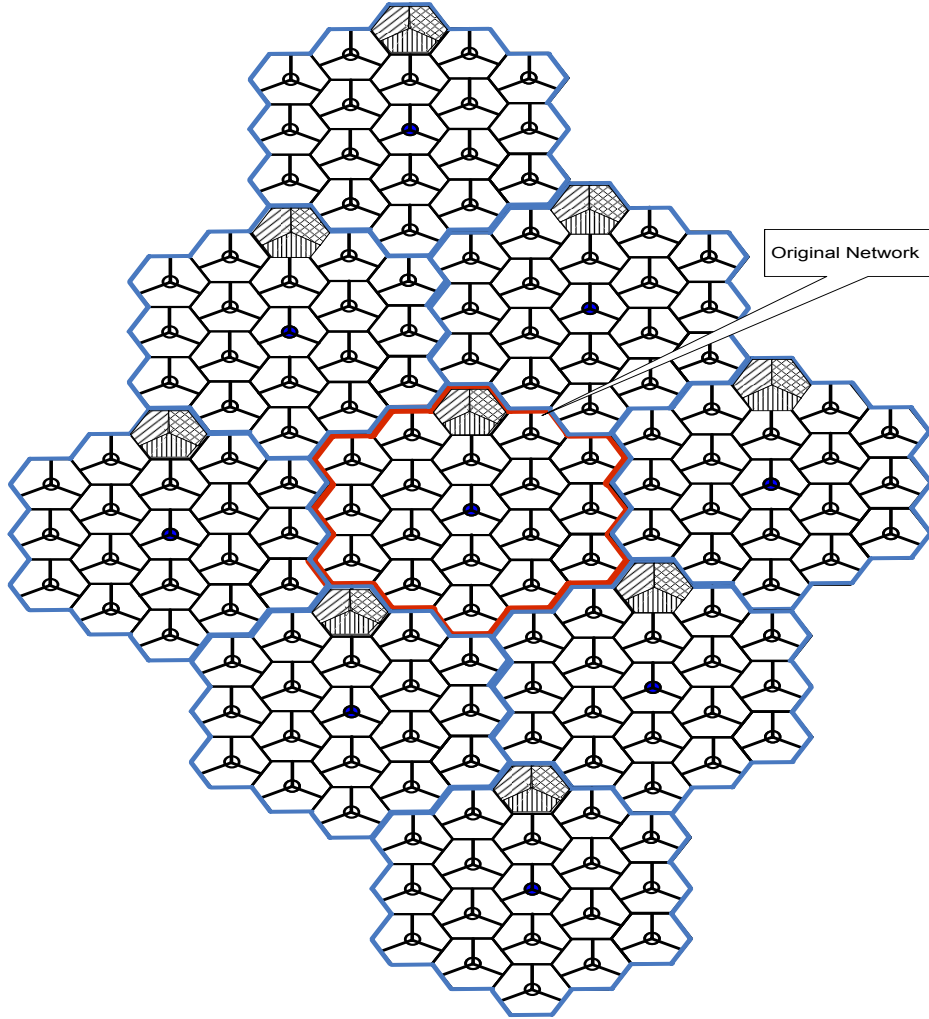where D is the distance between two neighboring BS.

Figure 3: An example of wraparound network.

3.4 Antenna Pattern

Antenna pattern for simulations has been referred from [3]. According to [3], all BS antenna elements have the beam pattern defined by 3GPP2. It is given by the formula:

$$G(\theta) = G_{max} + \max\left[-12\left(\frac{\theta}{\theta_{3dB}}\right)^2, -G_{FB}\right]$$

where

G_{max} in (dBi) is the maximum antenna gain (i.e. in the boresight direction).

θ is the angle (in degrees) of arrival relative to boresight with $|\theta| \leq 180$.

θ_{3dB} is the 3dB beam width (in degrees). It equals 70° in 3GPP antenna pattern [3].

G_{FB} is the front-to-back ratio in dBi (=25 dBi [3]). G_{FB}=0 for omni-directional antennas.

3.5 Shadowing and Fast Fading

The basic unit in an IEEE 802.16e based system is a slot. A slot is always defined as one subchannel by variable number of OFDM symbols (depending upon type of subcarrier distribution). A subchannel is further composed of a set of subcarriers. Since $SINR_{eff}$ is computed over a group of subcarriers, for WiMAX simulations we have calculated it over a slot. Shadowing is lognormal and its value has been kept constant over all the subcarriers of a slot. Since all sector antennas of a cell are co-located (i.e. at the center) and shadowing is caused by large obstacles in the signal path, SS will observe the same value of shadowing from all sectors of a specific cell. Fast fading is considered to follow Rayleigh distribution and it is supposed to change from one subcarrier to the other. This supposition is based on the fact that subcarriers of PUSC subchannel are randomly distributed in the available

bandwidth. It is drawn separately for every sector (if present). Fast fading and shadowing over a slot are shown in Fig.4.
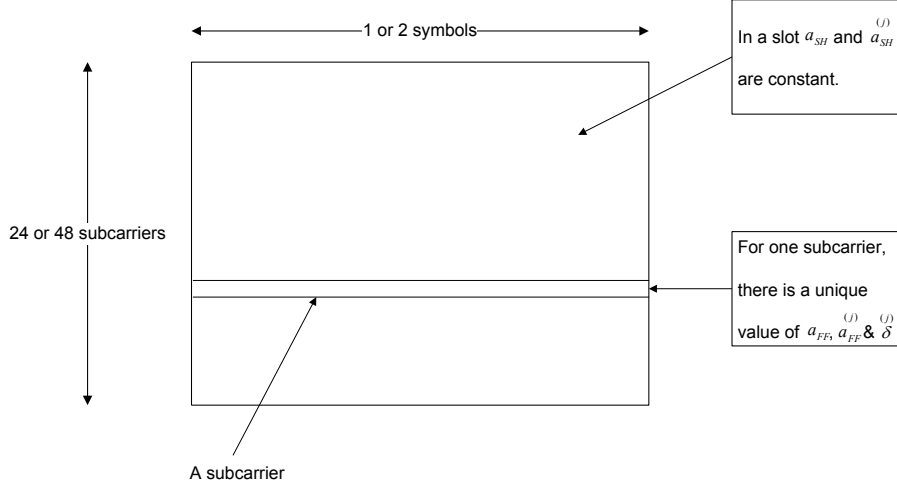
Figure 4: Shadowing and fast fading over a slot.

3.6 SS Spatial Distribution and Selection of Serving BS

SS is dropped into the cell using uniform random distribution. There are total three SS dropped into a cell. If the cell is sectorized, each sector has exactly one SS. Since we are using wraparound technique, three SS are dropped into every cell of the network.

There are two ways by which a SS can attach itself to a BS: minimum distance or best link. Since best link is more close to practical scenario, it is being employed in the simulations. For each SS, signal strength is measured from all the cells/sectors in the network. The SS selects the cell/sector from which it receives the maximum signal strength. The rest of the cells/sectors are the interfering ones (depending on the reuse pattern). Shadowing effect is taken into account during this procedure. However, fast fading is not considered during serving BS selection. The reason being that SS measures the signal from BS over sufficient interval of time to average out the fading effect.

13

3.7 Simulation Parameters

Simulation parameters are listed in Tab-1. These values are mainly based on [3].It is to be noted that value of BW_T used in simulations does not correspond to any FFT size. However, this bandwidth is divided into three equal parts (each of 5MHz) which corresponds to 512-FFT. It is done to gain flexibility in allocating a bandwidth to a cell/sector for every reuse pattern. If 10 MHz is assigned to a cell, it does not mean that 1024-FFT is employed, rather two unique parts (of 5 MHz each) with 512-FFT are attributed to the cell. P_{TX} of Tab-1 is the power transmitted by BS on all used subcarriers (data+pilot) in a cell. Power transmitted on one subcarrier is given by following expression:

$$P_{n,Tx} = \begin{cases} \frac{P_{Tx}N_f}{N_s N_{Sc}} & \text{for sectorized cells;} \\[2ex] \frac{P_{Tx}N_c}{N_s N_{Sc}} & \text{for non-sectorized cells.} \end{cases} \tag{5}$$

It is clear from the above expression that subcarrier power may be different for all reuse patterns. A second scheme of subcarrier power allocation (with same subcarrier power for every reuse pattern) will be discussed in section-5.

In order to give a clear view of relationship between available bandwidth and reuse factor, let us divide the BW_T of Tab-1 into three equal but distinct parts of 5 MHz each such that $BW_1 = BW_2 = BW_3 =$5 MHz. For different reuse patterns, these bandwidth parts are allocated in different ways. For frequency reuse pattern 3 x 3 x 3, FUSC is not possible as it cannot be segmented. Fig.5 gives detail about bandwidth allocation for six reuse factors.

14

Parameter	Description	Value
f	Carrier frequency	2.5 GHz
P_{TX}	Total rms transmit power of a cell	43dBm
$\frac{K}{d^\alpha}$	Pathloss model	COST-HATA-231, α=3.5, K=1.4 x 10^4
N_F	Number of OFDMA symbol in a frame	47
N_{DL}	Number of DL data OFDMA symbols	30
R_{DLUL}	DL to UL OFDMA symbols' ratio	2:1
BW_T	System bandwidth	15MHz
FFT Size	Total number of available subcarriers (with BW=5MHz)	512
N_{Sc}	Total number of used subcarriers (data+pilot) corresponding to BW_T	1260
N_{Sch}	Total number of used subchannels corresponding to BW_T	45
σ_{SH}	Log normal shadowing standard deviation	9 dB
$\triangle f$	Subcarrier spacing	10.9375 kHz
T_S	OFDMA useful symbol duration	91.43 μsec
T_{FR}	Frame Duration	5 ms
N_0	Thermal noise density	-174 dBm/Hz
R	One side of hexagonal cell	1Km
θ_{3dB}	3dB antenna beam width	70°
G_{FB}	Front-to-back antenna power ratio	25dBi
$LoadFactor$	Percentage of load (no. of used subchannels)	Eq.4

Table 1: Description and values of parameters used in simulations.

1 x 3 x 1

BW$_T$ BW$_T$
BW$_T$
BW$_T$ BW$_T$
BW$_T$ BW$_T$
BW$_T$

1 x 3 x 3

BW$_1$ BW$_2$
BW$_3$
BW$_1$ BW$_2$
BW$_1$ BW$_2$
BW$_3$
BW$_3$

1 x 1 x 1

BW$_T$
BW$_T$
BW$_T$

3 x 1 x 1

BW$_1$
BW$_2$
BW$_3$

3 x 3 x 1

BW$_1$ BW$_1$
BW$_1$
BW$_2$ BW$_2$
BW$_3$ BW$_3$
BW$_2$
BW$_3$
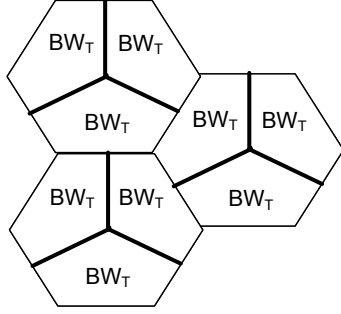
3 x 3 x 3
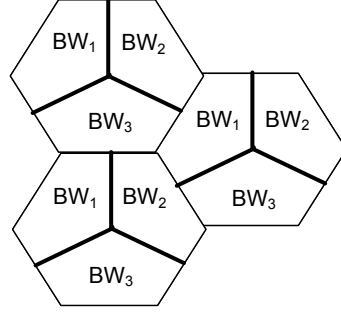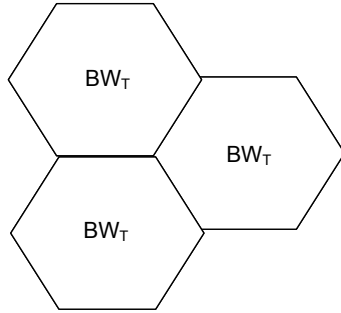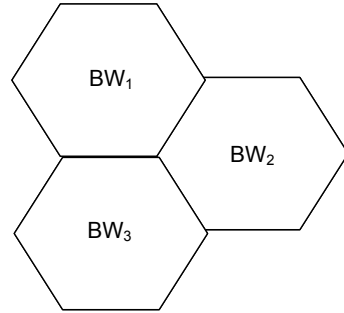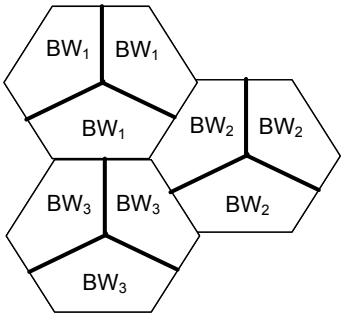
BW$_1$/3 BW$_1$/3
BW$_1$/3
BW$_2$/3 BW$_2$/3
BW$_3$/3 BW$_3$/3
BW$_2$/3
BW$_3$/3
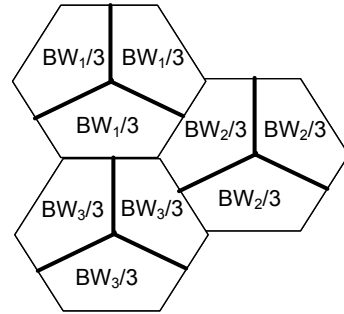
Figure 5: An example of bandwidth allocation for six different reuse factors.

16

4 Comparison of Reuse Patterns

4.1 Introduction

In this section simulation results are presented and analyzed. A good comparison for all six reuse patterns can be obtained by plotting a parameter for all the patterns in a single figure. But so many curves will mingle up and it will be difficult to carry out the comparison. Average $SINR_{eff}$ for three reuse patterns are plotted together on the same figure. Same is the case for average capacity. Results for each parameter are presented in different subsections. Parameters are only being plotted for PUSC since objective is to study the reuse pattern effect rather than to compare PUSC and FUSC.

4.2 $SINR_{eff}$ versus distance

In this subsection $SINR_{eff}$ versus distance plots are presented. To calculate $SINR_{eff}$ physical abstraction model MIC has been used. It is computed over subcarriers of a slot. Curves for reuse patterns having values $N_c = 1$ and $N_c = 3$ are grouped together on two different plots.
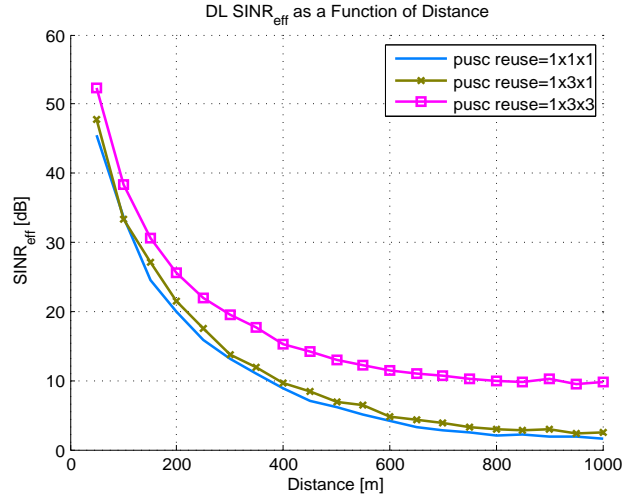
Figure 6: Avg. $SINR_{eff}$ vs distance for reuse 1x1x1, 1x3x1 and 1x3x3.
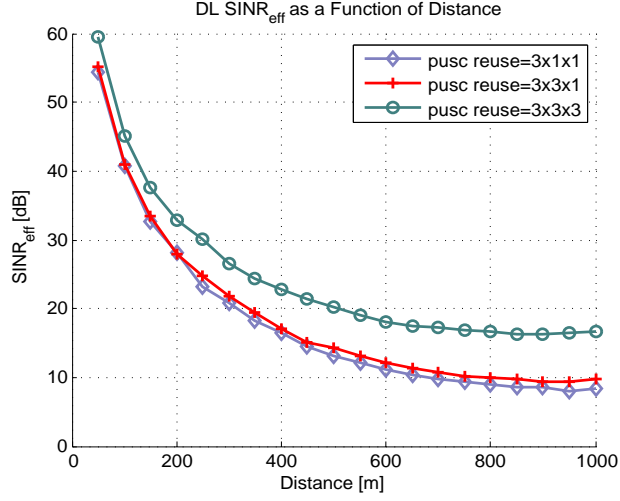
Figure 7: Avg. $SINR_{eff}$ vs distance for reuse 3x1x1, 3x3x1 and 3x3x3.

Results of plots for $SINR_{eff}$ versus distance are concluded in Tab-2:

Sequence w.r.t average values	Reuse pattern	Average $SINR_{eff}$ (dB)
1 (highest)	3 x 3 x 3	19.8
2	3 x 3 x 1	13.5
3	1 x 3 x 3	13.0
4	3 x 1 x 1	12.7
5	1 x 3 x 1	6.7
6 (lowest)	1 x 1 x 1	5.6

Table 2: Average values of $SINR_{eff}$ for six reuse patterns.

The average $SINR_{eff}$ values imply that reuse pattern 3 x 3 x 3 is the best choice. But MCS/$SINR_{eff}$ distributions also depend upon values of $SINR_{eff}$. Therefore we shall proceed with analysis of these distributions and conclude our result for effect of reuse patterns on $SINR_{eff}$.

4.3 MCS Distribution

In this subsection MCS distribution bar charts are given. The probability that a given SS will be eligible for a certain MCS type can be made out from these bar charts. Bar charts are being plotted separately for every reuse pattern. Tab-3 lists required threshold values of $SINR_{eff}$ for seven different MCS types [9]. Outage is also considered as one of the MCS types. A SS is said to be in outage if its radio conditions are so bad that it cannot receive anything.

Index	1	2	3	4	5	6	7
MCS	outage	QPSK 1/2	QPSK 3/4	16QAM 1/2	16QAM 3/4	64QAM 1/2	64QAM 3/4
$SINR_{th}$ **[dB]**	< 2.9dB	2.9	6.3	8.6	12.7	13.8	18

Table 3: Threshold of SINR values ($SINR_{th}$) for different MCS types [9].
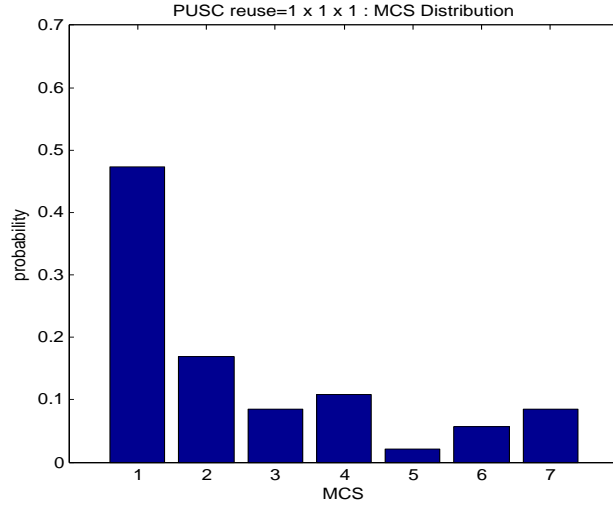
Figure 8: MCS distribution for reuse 1x1x1.
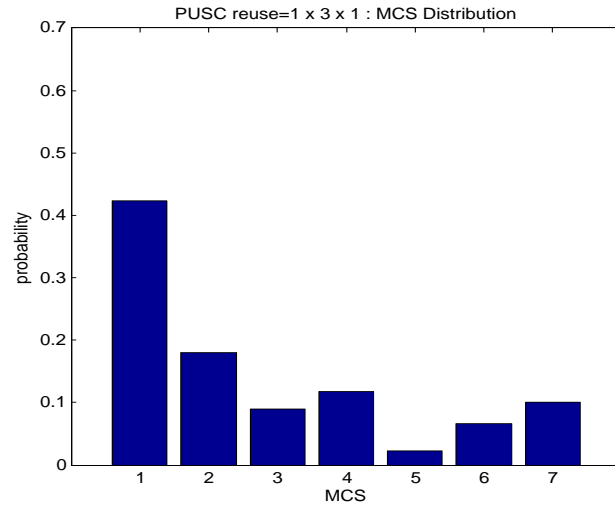
Figure 9: MCS distribution for reuse 1x3x1.
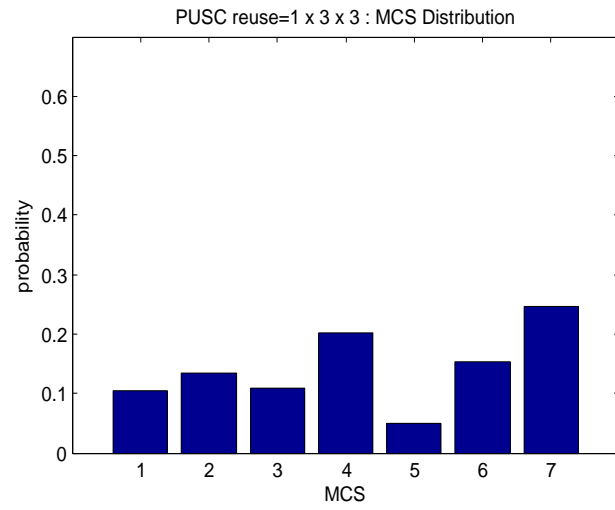
Figure 10: MCS distribution for reuse 1x3x3.
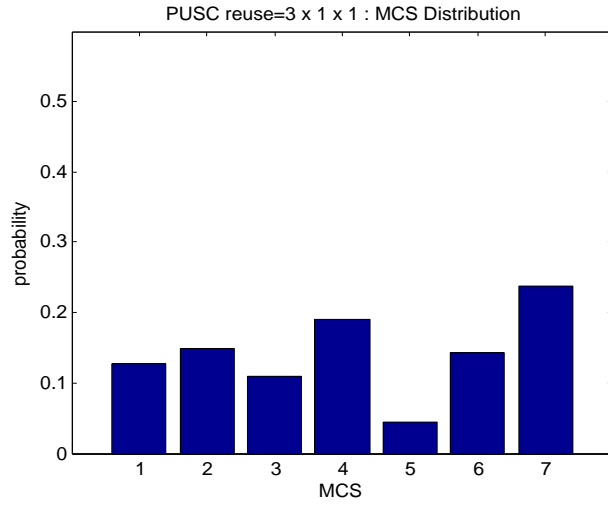
Figure 11: MCS distribution for reuse 3x1x1.
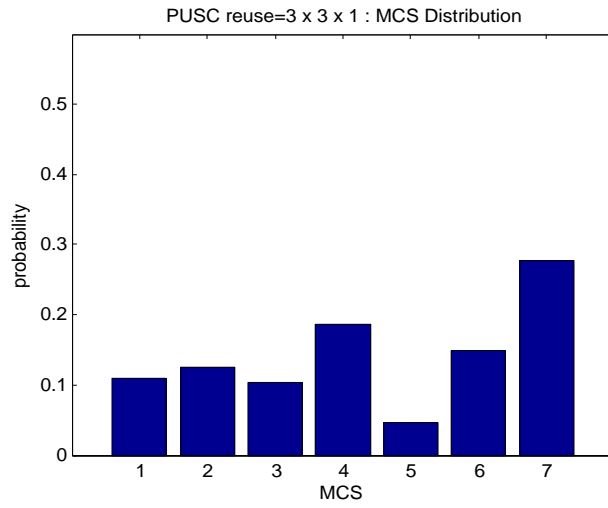
Figure 12: MCS distribution for reuse 3x3x1.
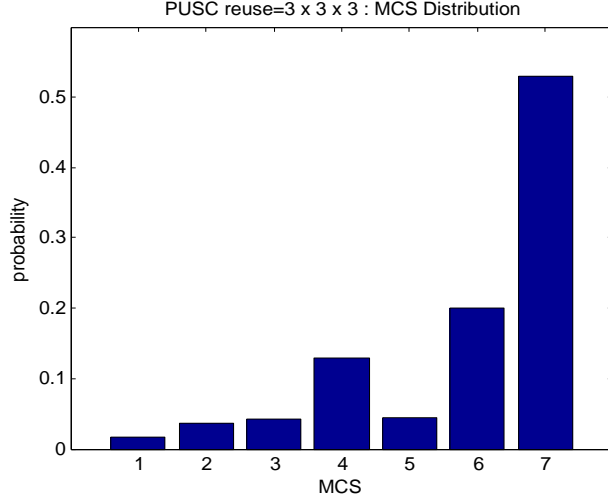
Figure 13: MCS distribution for reuse 3x3x3.

It is clear from the MCS distributions that reuse pattern 3 x 3 x 3 has the lowest outage probability and it has the highest value of probability for the MCS type '7'. Even after evaluation of MCS distribution results, reuse pattern 3 x 3 x 3 defends itself to be the best choice. The next parameter related to $SINR_{eff}$ is $SINR_{eff}$ distribution. It is being analyzed in the coming subsection.

4.4 $SINR_{eff}$ **Distribution**

This subsection contains $SINR_{eff}$ distributions. The Probability Density Function (PDF) are being plotted separately for every reuse pattern. An investigation is being carried out to identify a suitable distribution fit (of known distributions). The estimated parameters for this distribution are tabulated at the end of this subsection.

Figure 14: $SINR_{eff}$ Distribution for reuse 1x1x1.
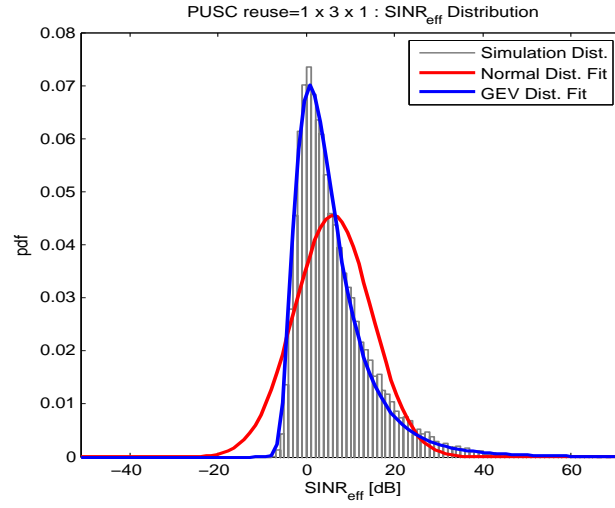
Figure 15: $SINR_{eff}$ Distribution for reuse 1x3x1.
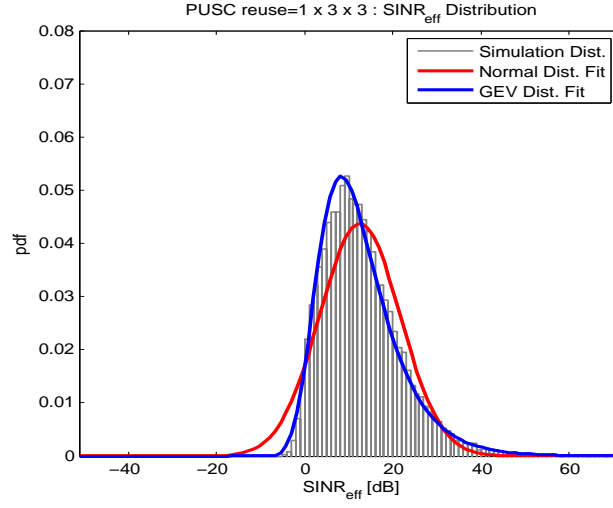
Figure 16: $SINR_{eff}$ Distribution for reuse 1x3x3.
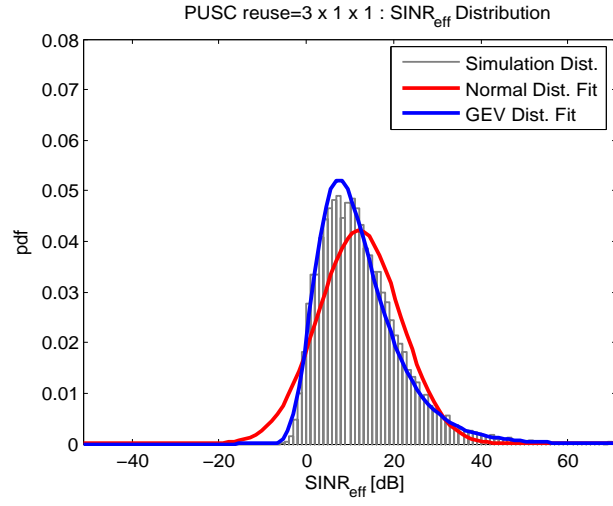
Figure 17: $SINR_{eff}$ Distribution for reuse 3x1x1.
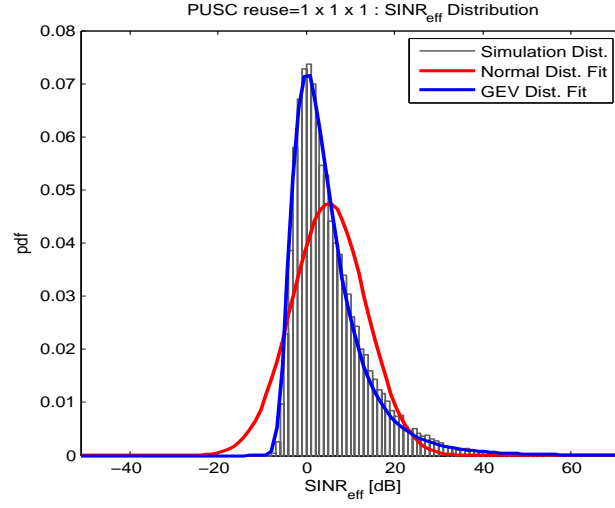
24
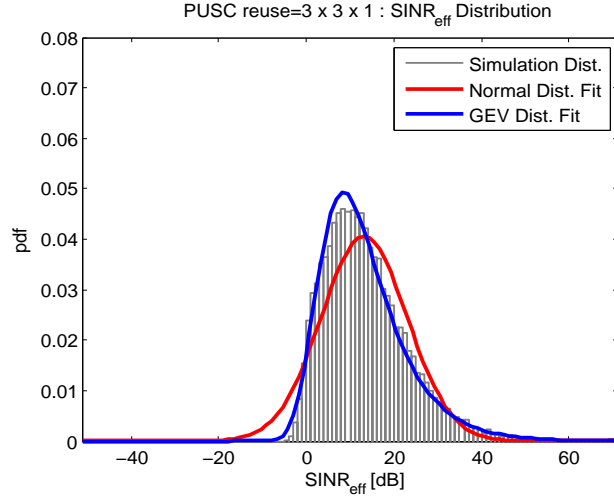
Figure 18: $SINR_{eff}$ Distribution for reuse 3x3x1.
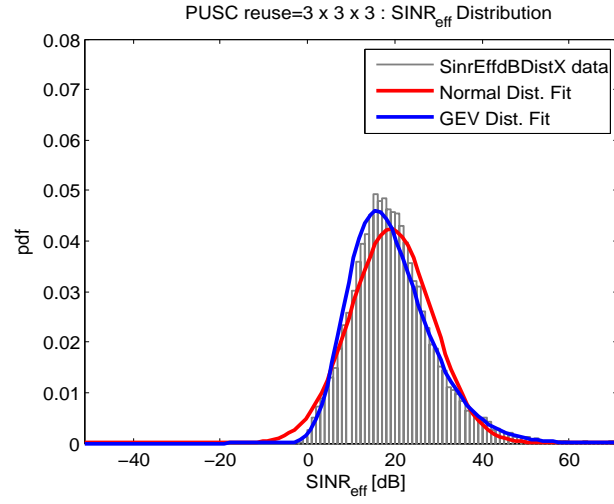
Figure 19: $SINR_{eff}$ Distribution for reuse 3x3x3.

A distribution fit has been tried for all $SINR_{eff}$ distribution plots. The known distribution types considered were: normal and extreme value and Generalized Extreme Value (GEV). The two distributions resulted in almost the same fitting parameters but GEV had better log likelihood values. In Tab-4 the parameters of distribution fits, obtained with normal and generalized extreme value distributions, are given.

Reuse Pattern	Normal Distribution		Generalized Extreme Value Distribution [8]				
	Mean	St. Deviation	Mean	St. Deviation	μ_{GEV}	σ_{GEV}	k_{GEV}
1 x 1 x 1	5.1	8.4	5.1	9.2	.98	5.2	0.19
1 x 3 x 1	6	8.8	6.1	9.7	1.7	5.3	0.20
1 x 3 x 3	12.5	9.1	12.5	9.1	8.4	7.0	0.02
3 x 1 x 1	12.1	9.5	12.1	9.6	7.7	7.0	0.043
3 x 3 x 1	13.2	9.8	13.2	9.9	8.7	7.5	0.026
3 x 3 x 3	19.2	9.4	19.2	9.4	15.1	8.0	-0.07

Table 4: Parameters of distribution fit.

As we analyze these parameters, the difference between mean/variance values of two distributions is not much. The reuse factor 3 x 3 x 3 has the highest value of mean and its value of variance is comparable to the rest of the variance values. Hence, the reuse pattern 3 x 3 x 3 delivers the best results for all three $SINR_{eff}$ related analyses.

Three more parameters of GEV distribution, μ_{GEV}, σ_{GEV} and shape parameter k, also appear in Tab-4. It is to be noted that μ_{GEV} and σ_{GEV} are not the distribution mean and standard deviation respectively. In the context of current analysis, it is not desirable to present more details on these parameters. However, interested reader can find complete details in [8]. After finishing with analysis of $SINR_{eff}$, we now examine the performance of six reuse patterns w.r.t cell capacity.

4.5 Capacity versus distance

In this subsection capacity versus distance curves are presented. Capacity is calculated for total available bandwidth in a cell. Curves for reuse patterns having values $N_c = 1$ and $N_c = 3$ are grouped together on two different plots.
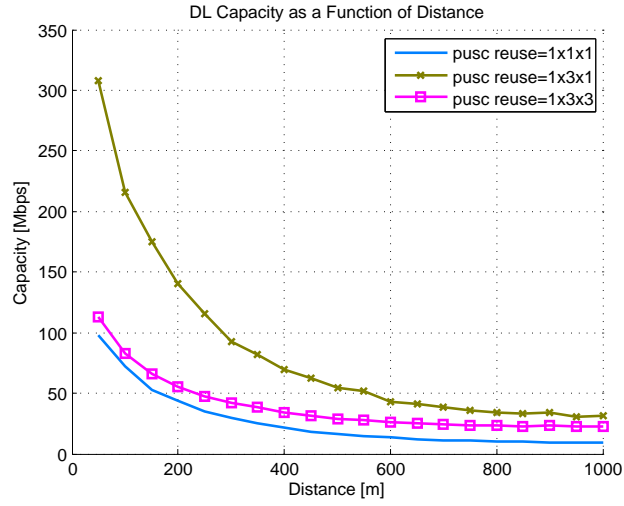
Figure 20: Avg. capacity vs distance for reuse 1x1x1, 1x3x1 and 1x3x3.
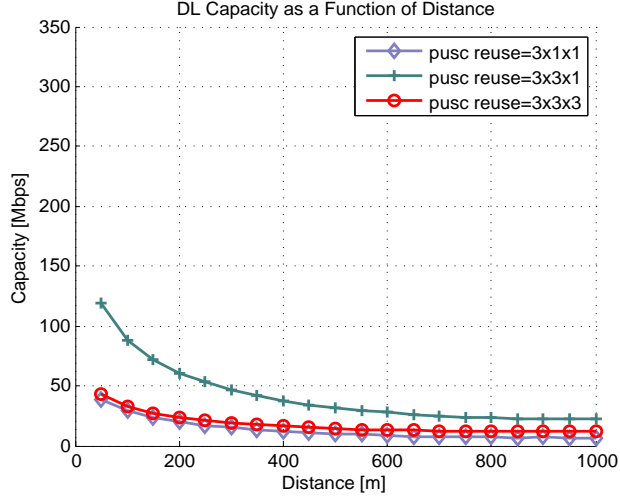
Figure 21: Avg. capacity vs distance for reuse 3x1x1, 3x3x1 and 3x3x3.

Results of plots for cell capacity versus distance are concluded in Tab-5:

Sequence w.r.t average values	Reuse pattern	Average capacity (Mbps)
1 (highest)	1 x 3 x 1	54.4
2	3 x 3 x 1	30.5
3	1 x 3 x 3	29.3
4	1 x 1 x 1	16.4
5	3 x 3 x 3	14.3
6 (lowest)	3 x 1 x 1	9.6

Table 5: Average values of capacities for six reuse patterns.

The average values of capacities show a total different picture. Reuse factor 3 x 3 x 3, which had the best results for $SINR_{eff}$ analysis, is placed very low in the list of average values of capacities. On the other hand, 1 x 3 x 1 has the highest value of average capacity. But it lagged performance in case of $SINR_{eff}$ analysis. Hence one reuse pattern delivering good results for $SINR_{eff}$, does not perform good in case of capacity analysis. The same is true for vice versa. To find a compromised choice, it is necessary to have an

overall picture of results. Therefore in next subsection all simulation results are put together.

4.6   Conclusion

The Tab-6 includes all the simulation results. It was concluded in subsection-4.4 that Normal and GEV distribution fits did not differ much in terms of mean and variance values. Also variance did not play a significant role in the conclusion. Therefore, in Tab-6, only mean values with GEV distribution fit are listed. As far as MCS distribution is concerned, it is important to have a look on outage probability. Hence it is also given in this table.

Reuse Pattern	Average $SINR_{eff}$ (dB)	$SINR_{eff}$ Distribution Mean	Outage Probability	Average Capacity (Mbps)
1 x 1 x 1	5.6	5.5	0.47	16.4
1 x 3 x 1	6.7	6.3	0.41	54.4
1 x 3 x 3	13.0	12.5	0.10	29.3
3 x 1 x 1	12.7	12.2	0.13	9.6
3 x 3 x 1	13.5	13.1	0.11	30.5
3 x 3 x 3	19.8	19.3	0.02	14.3

Table 6: Summary of simulation results.

Reuse patterns 1 x 1 x 1 and 1 x 3 x 1 have more than 40% outage probability which is unacceptable. Hence we shift our focus towards rest of four. 1 x 3 x 3 and 3 x 3 x 1 have almost same outage probability but latter has better performance for rest of the outcomes. Hence we drop 1 x 3 x 3 and move on to rest of three. 3 x 1 x 1 has low value of average capacity (as compared to other two) and a significant outage probability. It is also dropped and we are rest with two choices. Out of the last two, 3 x 3 x 1 provides a good trade off between capacity and $SINR_{eff}$ values but 11% outage probability is also objectionable. We therefore conclude and propose that 3 x 3 x 3 can be chosen as a reuse pattern for WiMAX cellular network. But if we relax the condition of outage probability a bit, 3 x 3 x 1 will be a good choice.

5 Effect of Cell Range and Subcarrier Power

In section-4, it was concluded that reuse patterns are easily knocked out on the basis of outage probabilities. In this section we shall try to investigate if these outage probabilities could be somehow reduced. For this purpose the effect of change in the values of cell range and subcarrier power are analyzed in this section. The outputs observed are average $SINR_{eff}$, outage probability and average capacity.

In section-4, the cell range was fixed as 1000 meters and subcarrier power was dependent upon reuse pattern. Here we shall see the influence of changing the cell range and subcarrier power. Rest of the parameters remain the same as were used in section-4.

5.1 Cell Ranges 500-1500m

The results for cell ranges 500, 750, 1000, 1250 and 1500 meters are presented in Tab-8,9,10. Two types of subcarrier power schemes are also compared in these tables. Apart from the power scheme used in section-4 (i.e. reuse pattern dependent subcarrier power), a second type is introduced here. For this second type subcarrier power is considered to be equal for every reuse pattern. For this purpose, reuse pattern 1 x 1 x 1 has been kept as a reference and complete transmission power, $P_{TX} = 43$ dBm, is allocated to each segregated part of BW_T. Since there are three distinct parts of BW_T (of 5 MHz each) used in a cell for reuse pattern 1 x 1 x 1, total cell power is equal to

$3 \times P_{TX}$. The subcarrier power for all reuse patterns is thus given as:

$$P'_{n,Tx} = 3 \times P_{Tx}/N_{Sc} \tag{6}$$

It is obvious from above expression that in contrast to Eqn-5 of section-3, subcarrier power for second power scheme is not dependent on a reuse pattern. It is calculated for reuse pattern 1 x 1 x 1 and then same is used for all other reuse patterns. The cell power for each reuse pattern for this second scheme can be found using expression:

$$P'_{Tx} = \frac{3P_{Tx}N_s}{N_f N_c} \tag{7}$$

The cell/subcarrier power for two subcarrier power schemes are listed in Tab-7. The first scheme in the tables is expressed as 'Constant cell power' and the second one as 'Constant subcarrier power'.

Reuse pattern	Cell/Sc power [dBm]			
	Constant cell power		Constant Sc power	
	Cell power	Sc power	Cell power	Sc power
1 x 1 x 1	43.0	12.0	47.8	16.7
1 x 3 x 1	43.0	7.2	52.5	16.7
1 x 3 x 3	43.0	12.0	47.8	16.7
3 x 1 x 1	43.0	16.7	43.0	16.7
3 x 3 x 1	43.0	12.0	47.8	16.7
3 x 3 x 3	43.0	16.7	43.0	16.7

Table 7: Cell/Subcarrier power for two power schemes.

| Reuse Type | Average $SINR_{eff}$ [dB] | | | | | | | | | |
| | Cell Range= 500m | | Cell Range= 750m | | Cell Range= 1000m | | Cell Range= 1250m | | Cell Range= 1500m | |
	Const Pr/cell	Const Pr/Sc	Const Pr/cell	Const Pr/Sc	Const Pr/cell	Const Pr/Sc	Const Pr/cell	Const Pr/Sc	Const Pr/cell	Const Pr/Sc
1 x 1 x 1	5.5	5.6	5.7	5.7	5.6	5.7	5.7	5.6	5.6	5.6
1 x 3 x 1	6.7	6.5	6.6	6.8	6.7	6.7	6.5	6.8	6.2	6.7
1 x 3 x 3	13.0	13.1	13.2	13.2	13.0	13.1	12.9	13.0	12.4	12.9
3 x 1 x 1	12.6	- - -	12.7	- - -	12.7	- - -	12.5	- - -	12.5	- - -
3 x 3 x 1	13.9	13.8	13.7	13.8	13.5	13.8	13.3	13.7	13.0	13.6
3 x 3 x 3	20.0	- - -	20.0	- - -	19.8	- - -	19.4	- - -	19.1	- - -

Table 8: Avg. $SINR_{eff}$ values for two power per subcarrier schemes

| Reuse Type | Outage Probability | | | | | | | | | |
| | Cell Range= 500m | | Cell Range= 750m | | Cell Range= 1000m | | Cell Range= 1250m | | Cell Range= 1500m | |
	Const Pr/cell	Const Pr/Sc	Const Pr/cell	Const Pr/Sc	Const Pr/cell	Const Pr/Sc	Const Pr/cell	Const Pr/Sc	Const Pr/cell	Const Pr/Sc
1 x 1 x 1	0.48	0.47	0.47	0.47	0.47	0.47	0.47	0.47	0.48	0.47
1 x 3 x 1	0.42	0.42	0.42	0.41	0.41	0.42	0.43	0.41	0.43	0.42
1 x 3 x 3	0.11	0.11	0.11	0.10	0.10	0.11	0.11	0.11	0.12	0.11
3 x 1 x 1	0.13	- - -	0.13	- - -	0.13	- - -	0.13	- - -	0.13	- - -
3 x 3 x 1	0.11	0.11	0.11	0.11	0.11	0.11	0.11	0.11	0.12	0.11
3 x 3 x 3	0.02	- - -	0.02	- - -	0.02	- - -	0.02	- - -	0.02	- - -

Table 9: Outage probability values for two power per subcarrier schemes

Reuse Type	Capacity [Mbps]									
	Cell Range= 500m		Cell Range= 750m		Cell Range= 1000m		Cell Range= 1250m		Cell Range= 1500m	
	Const Pr/cell	Const Pr/Sc	Const Pr/cell	Const Pr/Sc	Const Pr/cell	Const Pr/Sc	Const Pr/cell	Const Pr/Sc	Const Pr/cell	Const Pr/Sc
1 x 1 x 1	16.2	16.4	16.5	16.5	16.4	16.6	16.5	16.3	16.4	16.4
1 x 3 x 1	54.5	53.3	53.8	54.6	54.4	54.5	53.2	55.1	52.1	54.3
1 x 3 x 3	29.4	29.4	29.7	29.7	29.3	29.6	29.1	29.4	28.2	29.1
3 x 1 x 1	9.5	- - -	9.6	- - -	9.6	- - -	9.5	- - -	9.5	- - -
3 x 3 x 1	31.0	31.2	30.8	30.9	30.5	31.0	30.0	30.8	29.5	30.5
3 x 3 x 3	14.5	- - -	14.5	- - -	14.3	- - -	14.1	- - -	13.8	- - -

Table 10: Avg. Capacity values for two power per subcarrier schemes

It can be deduced from the results listed in Tables-8,9,10 that values are almost the same for cell ranges between 500-1500 meters. The small variations can be observed for cell range=1500 meters and that too with first power scheme only. However, the difference is not much as compared to the amount of power per cell increased for various reuse patterns. For reuse patterns 3 x 3 x 1 and 3 x 3 x 3 both the power schemes result in same subcarrier power hence values for only one power scheme are given in the above tables for these reuse patterns.

5.2 Cell Ranges 500-6000m

It was observed in subsection-5.1 that outputs does not change much for cell ranges (between 500 and 1500 meters) for all the reuse patterns. Therefore simulations were carried out over larger values of cell ranges. It was noticed that all reuse patterns showed similar variations in results over larger values of cell ranges. Here only the results for reuse pattern 3 x 3 x 3 and 3 x 3 x 1 are presented. The former reuse pattern outclassed the rest in terms of outage probability (section-4). It will be interesting to look for maximum cell range for which the outage probability remains less than five percent. However, for this reuse pattern the two power schemes result in the same value of cell power (Tab-7). To see the effect of both power schemes, results for reuse pattern 3 x 3 x 1 are also presented. For this reuse, the value of cell

power is different for two power schemes. MCS distributions for both reuse patterns are given in Fig-22,23.24.
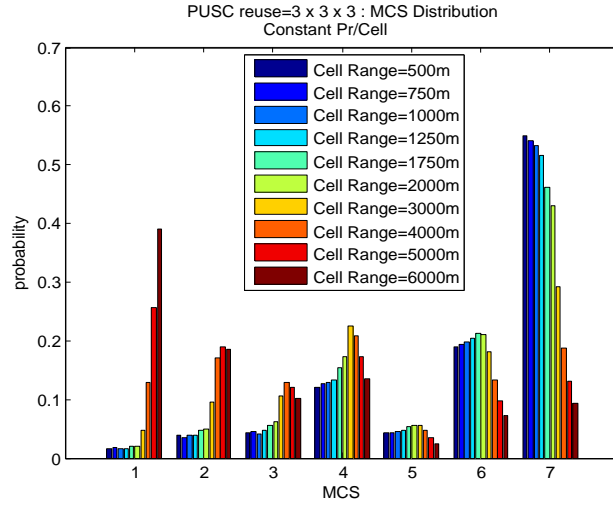
Figure 22: MCS distribution for different cell ranges.
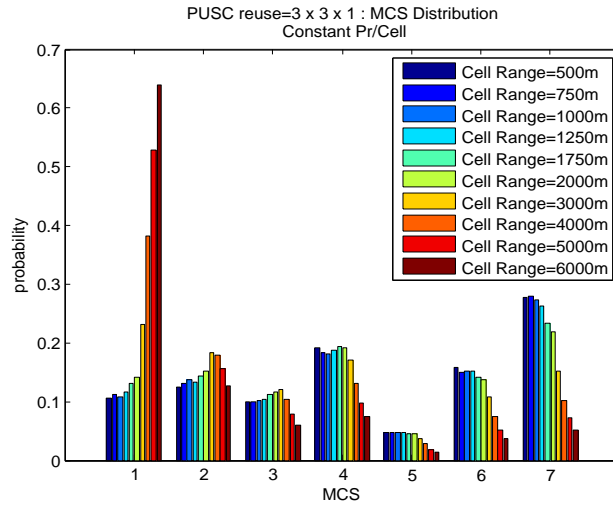
Figure 23: MCS distribution for different cell ranges with first power scheme.
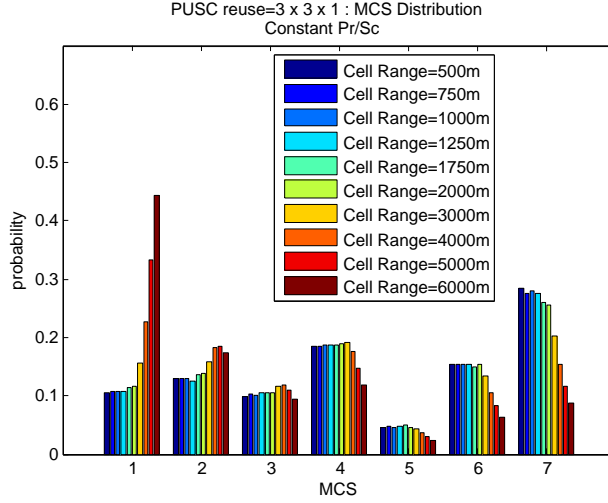
Figure 24: MCS distribution for different cell ranges with second power scheme.

It is clear from the plots of MCS distribution that there is a small change in the value of outage probability till cell range of 2000m. It increases significantly after that. However, for reuse 3 x 3 x 3 outage probability remains less than five percent (= 0.047) even with cell range of 3000m. In case of reuse 3x3x1, till cell range = 2000m, both power schemes result in almost the same values of outage probability. Beyond that cell range, second power scheme (with increased power per cell) gives relatively smaller values of outage probability than the first power scheme.

Next step is to check the variation in the average values of $SINR_{eff}$ with increasing distance from BS. The values plotted as a function of distance for both the reuse patterns with various cell ranges are presented in Fig-25,. For clarity some cell ranges in between are omitted.
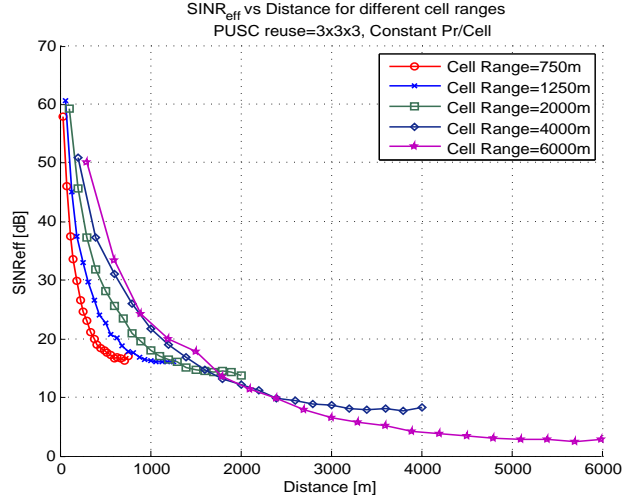
Figure 25: Avg. $SINR_{eff}$ vs distance for different cell ranges.
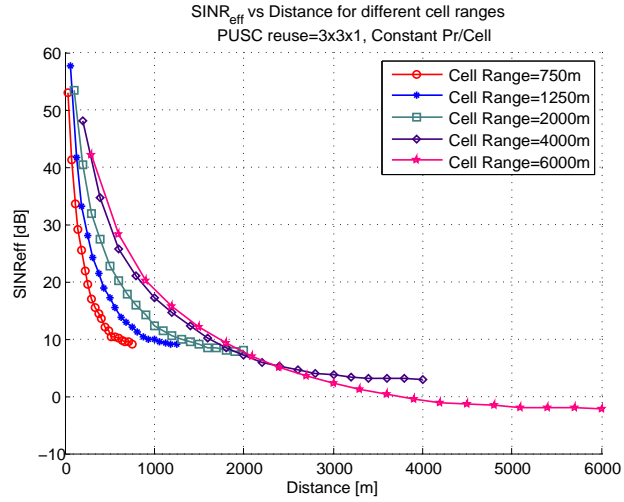
Figure 26: Avg. $SINR_{eff}$ vs distance for different cell ranges for first power scheme.

It is visible from the above plots that higher the value of cell range the higher is value of average $SINR_{eff}$ at a particular distance from the BS. But since the values of average $SINR_{eff}$ are quite low after 2000m, it becomes necessary to look for average $SINR_{eff}$ per cell for all cell ranges. Average capacities and values of outage probabilities for all cell ranges are also given in

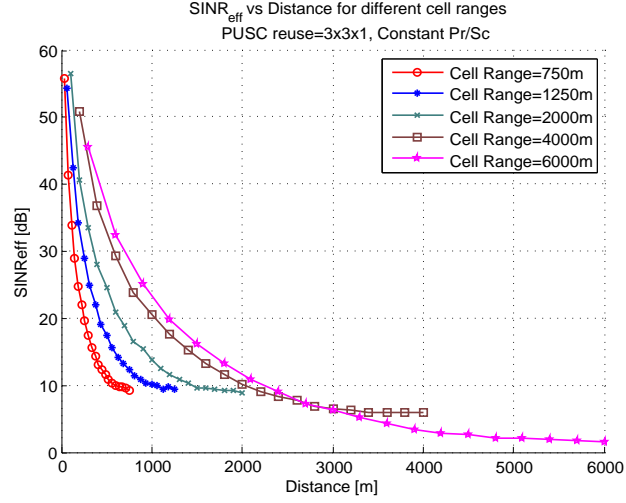Figure 27: Avg. $SINR_{eff}$ vs distance for different cell ranges for second power scheme.

Tab-11,12,13. For reuse 3 x 3 x 1, similar behavior is observed for two power schemes as was noticed in it's MCS distribution i.e. both power schemes give similar values till cell ranges 2000m and an increase in cell power (second power scheme) improves the performance at higher cell ranges.

Output Type	PUSC Reuse 3 x 3 x 1							
	Cell Range= 500m		Cell Range= 750m		Cell Range= 1000m		Cell Range= 1250m	
	Const Pr/cell	Const Pr/Sc	Const Pr/cell	Const Pr/Sc	Const Pr/cell	Const Pr/Sc	Const Pr/cell	Const Pr/Sc
Outage Probability	0.11	0.11	0.11	0.11	0.11	0.11	0.11	0.11
Avg $SINR_{eff}$[dB]	13.8	13.9	13.7	13.8	13.5	13.8	13.3	13.7
Avg Capacity[Mbps]	31.0	31.2	30.8	30.9	30.5	31.0	30.0	30.8
	PUSC Reuse 3 x 3 x 3							
Outage Probability	0.02	- - -	0.02	- - -	0.02	- - -	0.02	- - -
Avg $SINR_{eff}$[dB]	20.0	- - -	19.8	- - -	19.8	- - -	19.4	- - -
Avg Capacity[Mbps]	14.5	- - -	14.4	- - -	14.3	- - -	14.0	- - -

Table 11: PUSC Reuse 3 x 3 x 1 Cell Ranges: 500,750,1000,1250m

Output Type	PUSC Reuse 3 x 3 x 1					
	Cell Range= 1750m		Cell Range= 2000m		Cell Range= 3000m	
	Const Pr/cell	Const Pr/Sc	Const Pr/cell	Const Pr/Sc	Const Pr/cell	Const Pr/Sc
Outage Probability	0.13	0.11	0.14	0.12	0.23	0.16
Avg. $SINR_{eff}$ [dB]	12.6	13.2	12.1	13.2	9.6	11.6
Avg. Capacity [Mbps]	28.6	29.9	27.7	29.8	23.1	26.8
	PUSC Reuse 3 x 3 x 3					
Outage Probability	0.02	- - -	0.02	- - -	0.047	- - -
Avg. $SINR_{eff}$ [dB]	18.4	- - -	17.8	- - -	14.8	- - -
Avg. Capacity [Mbps]	13.4	- - -	13.0	- - -	10.9	- - -

Table 12: PUSC Reuse 3 x 3 x 1 Cell Ranges: 1750,2000,3000m

It is clear from the values listed in above tables that for both the power schemes, decrease in average $SINR_{eff}$/capacity and increase in outage probability is observed beyond cell range=1250m. The two power schemes give almost the same outputs till cell range=1250m. For cell range up to 1250m, the first one is better than the second one. The reason being that for the

Output Type	PUSC Reuse 3 x 3 x 1					
	Cell Range= 4000		Cell Range= 5000		Cell Range= 6000	
	Const Pr/cell	Const Pr/Sc	Const Pr/cell	Const Pr/Sc	Const Pr/cell	Const Pr/Sc
Outage Probability	0.38	0.23	0.52	0.33	0.63	0.44
Avg. $SINR_{eff}$ [dB]	6.8	9.7	4.1	7.6	1.7	5.6
Avg. Capacity [Mbps]	18.4	23.3	14.5	19.8	11.6	16.6
	PUSC Reuse 3 x 3 x 3					
Outage Probability	0.13	- - -	0.26	- - -	0.39	- - -
Avg. $SINR_{eff}$ [dB]	11.5	- - -	8.8	- - -	6.4	- - -
Avg. Capacity [Mbps]	8.8	- - -	7.2	- - -	5.9	- - -

Table 13: PUSC Reuse 3 x 3 x 1 Cell Ranges: 4000,5000,6000m

second power scheme the power per cell for certain reuse patterns is greater than that with the first scheme and this extra power results in no advantage. Though the reuse pattern 3 x 3 x 3 gives acceptable outage probability even with cell range=3000m but at the same time considerable decrease in the values of average $SINR_{eff}$ and capacity can be seen for this cell range.

5.3 Cell Powers 37-51 dBm

The two power schemes considered in subsection-10 resulted in variation of cell power values for various reuse patterns. However, results were compared for only two values of cell power for every reuse pattern (except 3 x 1 x 1 and 3 x 3 x 3). In this subsection the cell range is fixed and variations in the values of outage probability, average $SINR_{eff}$ and average capacity are evaluated over a considerable range of cell power values.

	Average $SINR_{eff}$ [dB] (cell range = 1500m)							
Cell power[dBm]	37	39	41	43	45	47	49	51
1 x 1 x 1	5.4	5.5	5.6	5.6	5.6	5.6	5.7	5.6
1 x 3 x 1	5.4	5.8	6.0	6.2	6.4	6.4	6.6	6.7
1 x 3 x 3	11.1	11.8	12.2	12.4	12.8	12.9	12.9	13.0
3 x 1 x 1	12.2	12.3	12.4	12.5	12.6	12.6	12.6	12.5
3 x 3 x 1	13.8	13.9	13.7	13.0	13.5	13.8	13.3	13.7
3 x 3 x 3	17.2	17.9	18.6	19.1	19.3	19.7	19.8	20.0

Table 14: Avg. $SINR_{eff}$ values for different cell powers.

	Average Capacity [Mbps] (cell range = 1500m)							
Cell power[dBm]	37	39	41	43	45	47	49	51
1 x 1 x 1	16.0	16.2	16.3	16.4	16.4	16.4	16.5	16.4
1 x 3 x 1	48.6	50.3	51.2	52.1	53.0	52.8	54.2	54.3
1 x 3 x 3	25.7	27.1	27.7	28.2	28.9	29.2	29.1	29.2
3 x 1 x 1	9.3	9.4	9.4	9.5	9.5	9.6	9.6	9.5
3 x 3 x 1	26.8	27.9	28.9	29.5	30.0	30.3	30.7	30.9
3 x 3 x 3	12.5	13.0	13.5	13.8	14.0	14.3	14.3	14.5

Table 15: Avg. Capacity values for different cell powers.

As can be seen from the above tables that reuse patterns 1 x 1 x 1, 3 x 1 x 1 and 3 x 3 x 1 appear less sensitive towards change in cell power values. While the other three reuse patterns show noticeable variations because of changes in cell power. The variations depict improvements with increase in cell power value. However, these improvements are quite small as compared to the amount by which cell power is increased.

5.4 conclusion

In this section the effect of different cell ranges and cell powers have been studied. It was concluded in subsection-5.2 that performance of reuse patterns diminishes significantly beyond 1250m. Hence it can be set as maxi-

Cell power[dBm]	Outage Probability (cell range = 1500m)							
	37	39	41	43	45	47	49	51
1 x 1 x 1	0.49	0.48	0.48	0.48	0.48	0.47	0.47	0.48
1 x 3 x 1	0.48	0.46	0.46	0.43	0.43	0.43	0.42	0.41
1 x 3 x 3	0.15	0.13	0.13	0.12	0.11	0.11	0.11	0.11
3 x 1 x 1	0.14	0.14	0.13	0.13	0.13	0.13	0.13	0.13
3 x 3 x 1	0.16	0.13	0.12	0.12	0.12	0.11	0.11	0.11
3 x 3 x 3	0.02	0.02	0.02	0.02	0.02	0.02	0.02	0.01

Table 16: Outage probability values for different cell powers.

mum allowable cell range. Increase in cell power values does not bring much improvement. Even for some reuse patterns there is no improvement at all. Hence cell power value being suggested in [3] can be considered as appropriate.

6   Conclusion

In this report a comprehensive comparison of six different reuse patterns has been presented. Radio quality and capacity analysis of these pattern has shown that reuse pattern 3 x 3 x 3 has an acceptable performance as compared to the rest. The limiting factor was outage probability. During further analysis, cell range and subcarrier power were changed and their effect on different reuse pattern was studied. All reuse patterns almost behaved the same towards these variations. Acceptable cell range was found to be 2000 m. Upto cell range of 2000 m, increase in cell power did not have any positive effect on radio quality or capacity. That is why both power schemes (constant cell power and constant subcarrier power) came up with the same results. Beyond cell range range of 2000m, increase in cell power showed improvement but that increase was not significant enough to justify the corresponding increase in cell power. Hence, it was concluded that cell range should not be increased beyond 2000 m.

References

[1] IEEE 802.16-2004, "IEEE Standard for Local and Metropolitan Area 200 Networks - Part 16: Air Interface for Fixed Broadband Wireless Access Systems", October 2004.

[2] IEEE Std. 802.16e, "IEEE Standard for local and metropolitan area networks, Part 16: Air Interface for Fixed and Mobile Broadband Wireless Access Systems, Amendment 2: Physical and Medium Access Control Layers for Combined Fixed and Mobile Operation in Licensed Bands and Corrigendum 1", May 2005.

[3] Wimax Forum, Krishna Ramadas and Raj Jain (contact persons for this document), "WiMAX System Evaluation Methodology", Jan 2007.

[4] J. Pons and J. Dunlop, "Enhanced System Level/Link Level Simulation Interface For Gsm", IEEE VTC Fall 99, Ottawa, pp. 1189 - 1193.

[5] David Huo, "Clarification on the Wrap-Around Hexagon Network Structure", IEEE 802.20 Working Group on Mobile Broadband Wireless Access, IEEE C802.20-05/15, Mar 2005.

[6] Jamshid Khun-Jush, "CDMA uplink Power Control Methodology in SEAMCAT (VOICE ONLY)", SEAMCAT Technical Group, STG(03)13 r1, Oct 2003.

[7] Masood Maqbool, Marceau Coupechoux and Philippe Godlewski; "Comparison of PHY Abstraction Models for IEEE 802.16e", Technical Report, Tlcom Paris, 2007.

[8] The MathWorks website, "Statistics Toolbox 6.0, Modelling Data with the Generalized Extreme Value Distribution", Jun 2007.
http://www.mathworks.com/products/statistics/demos.html?file=/products/demos/shipping/stats/gevdemo.html

[9] "WiMAX Forum Mobile System Profile 4 Release 1.0 Approved Specification", Wimax Forum, May 2007.